A first-principles study on the Rashba effect in surface systems

2009 J. Phys.: Condens. Matter 21 064239

(http://iopscience.iop.org/0953-8984/21/6/064239)

J. Phys.: Condens. Matter **21** (2009) 064239 (8pp) doi:10.1088/0953-8984/21/6/064239

A first-principles study on the Rashba effect in surface systems

Miki Nagano[1], Ayaka Kodama[1], T Shishidou[1] and T Oguchi[1,2]

[1] Department of Quantum Matter, ADSM, Hiroshima University, Kagamiyama, Higashihiroshima 739-8530, Japan
[2] Institute for Advanced Materials Research, Hiroshima University, Kagamiyama, Higashihiroshima 739-8530, Japan

E-mail: oguchi@hiroshima-u.ac.jp

Received 18 July 2008, in final form 1 September 2008
Published 20 January 2009
Online at stacks.iop.org/JPhysCM/21/064239

Abstract
The Rashba effect in several surface systems, Au(111), Au(110), Ag(111), Sb(111) and Si(111)–Bi, is studied by means of first-principles relativistic density-functional calculations. The importance of the asymmetric behavior around the surface atom is emphasized as a crucial factor to determine the magnitude of Rashba spin splitting in addition to the size of the spin–orbit coupling. The Rashba effect at the Brillouin-zone boundary is generally described with time-reversal symmetry. Distinctive features in the spin splitting and spin direction for a two-dimensional hexagonal system are discussed with the use of symmetry in the double group of k.

1. Introduction

The Rashba effect has originally been studied as a spin splitting phenomenon, where a free electron of spin $\boldsymbol{s}$ moves with momentum $\hbar\boldsymbol{k}$ under an electric field along the z direction [1]. The Rashba Hamiltonian is then given as

$$\mathcal{H}_{\mathrm{R}} = \alpha_{\mathrm{R}} \left(\hat{\boldsymbol{z}} \times \hbar\boldsymbol{k}\right) \cdot \boldsymbol{s}. \tag{1}$$

The corresponding eigenstate has spin quantized perpendicular to the field and the wavevector $\boldsymbol{k}$ on the xy plane. The Rashba effect in two-dimensional (2D) electron-gas systems has been extensively investigated and its possible applications to spin generation and control are highly expected for the next-generation spintronics devices.

The microscopic origin of the Rashba effect is known to be spin–orbit coupling (SOC), which is one of the relativistic effects and can be given in Ryd atomic units as

$$\mathcal{H}_{\mathrm{SOC}} = \frac{2}{c^2} (\nabla V \times \boldsymbol{p}) \cdot \boldsymbol{s}, \tag{2}$$

where V is a crystal potential, $\boldsymbol{p}$ is a momentum operator and c is the velocity of light ($c^{-2} = 1.33 \times 10^{-5}$). It is easily seen that SOC can be reduced to the Rashba Hamiltonian for a free-electron system with an external field. In the case of a spherically symmetric potential, a much more familiar expression can be obtained as

$$\mathcal{H}_{\mathrm{SOC}} = \frac{2}{c^2} \frac{1}{r} \frac{\mathrm{d}V(r)}{\mathrm{d}r} \boldsymbol{l} \cdot \boldsymbol{s} = \hat{\zeta} \boldsymbol{l} \cdot \boldsymbol{s}, \tag{3}$$

which is the direct representation of a coupling between spin and orbital ($\boldsymbol{l}$) angular momentum operators. As discussed below, the spherically symmetric term around each atom is usually relevant because of the dominant contribution from a nucleus charge to the potential gradient.

An SOC-origin spin splitting may often be seen in the case of a non-centrosymmetric system with large SOC. For bulk states it is called the Dresselhaus effect [2] while for surface states it is also known as the Rashba effect. A Rashba spin splitting has actually been observed by the angle-resolved photoemission spectroscopy (ARPES) technique for heavy-element surfaces such as Au(111) [3–5]. Recently, the Rashba effect has been studied for many surface systems both experimentally [6–11] and theoretically [12–16].

In this study, the surface states for some surface systems, Au(111), Ag(111) and Sb(111), are investigated by first-principles electronic-structure calculations with the inclusion of SOC. By comparing the Rashba splitting for the different surface systems, it is found that asymmetric features of the surface state in the nucleus region at the surface atom are crucial to determine the magnitude of the splitting in addition to the size of the SOC. To study a variation in the Rashba effect

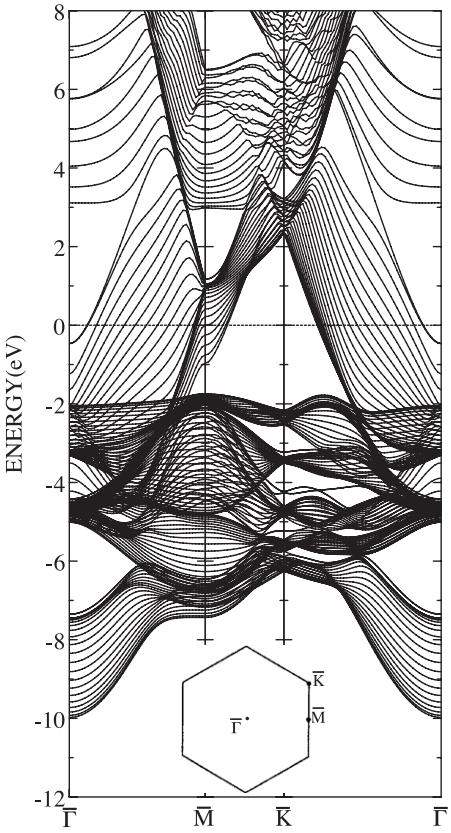

Figure 1. Electronic band structure of the Au(111) 23-layer slab model calculated without spin–orbit coupling along the two-dimensional hexagonal Brillouin zone (inset). The Fermi energy is set to the origin of energy.

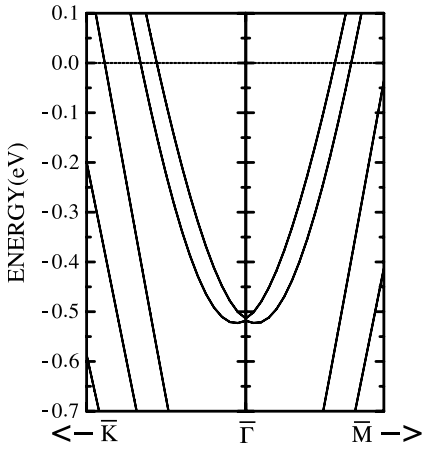

Figure 2. Electronic band structure of Au(111) calculated with spin–orbit coupling around $\bar{\Gamma}$. Boundaries plotted are $(1/15, 1/15)(2\pi/a)$ on $\bar{\Gamma}\bar{K}$ and $(1/10, 0)(2\pi/a)$ toward $\bar{\Gamma}\bar{M}$, being 1/5 the size of the full zone. The Fermi energy is set to the origin of energy.

at a surface, the electronic structure of the Au(110) surface is also calculated by assuming (1 × 1) and (2 × 1) surface structures. Calculated results for Au(110) are compared with an ARPES experiment [17, 18]. An adsorbed surface system is also investigated for Si(111)-($\sqrt{3} \times \sqrt{3}$)–Bi. In the Si(111)–Bi system, Rashba-type spin splitting is obtained not only at the zone center ($\bar{\Gamma}$) but also at the high-symmetry k points ($\bar{M}$ and $\bar{K}$) on the 2D Brillouin-zone (BZ) boundary, being consistent with the results of a recent ARPES measurement [19]. General aspects of the Rashba spin splitting at the zone boundary and the resultant spin direction are discussed in detail.

2. Methods and models

Our calculations are based on the first-principles density-functional approach. One-electron Kohn–Sham equations are solved with the all-electron full-potential linear augmented-plane-wave (FLAPW) method and SOC is included as a second variation in self-consistent-field iterations.

In order to simulate surface systems, a repeated slab model is adopted in the present calculations. Since the size of the Rashba splitting is often very small, like of the order of meV, the thickness of the slab model used should be checked to eliminate the interaction between the surface states on both sides. It is known for semiconductor surfaces that the dangling bonds on the back side can be terminated by putting hydrogen atoms there. However, no such termination scheme is available for metallic surfaces. This may be because a dangling bond to be terminated is not clearly formed in metallic systems. We have tested the band splitting due to the surface-state interaction by changing the slab thickness for Au(111), Au(110) and Ag(111) and have found that a 23-layer thickness is sufficient to get the undesired splitting to less than 10 meV. For Sb(111), a 12-layer model is enough to get the same accuracy. As for the Si(111)-($\sqrt{3} \times \sqrt{3}$)–Bi surface system, a 12-layer slab with hydrogen termination is used. Possible adsorption sites of Bi are known to be T_4 and H_3 on Si(111) and the former is believed to be more stable than the latter [20–23]. We first have optimized the structure of Si(111)-($\sqrt{3} \times \sqrt{3}$)–Bi for both T_4 and H_3 adsorption sites, compared the total energy between them and confirmed the relative stability of the T_4 site (see figure 9). This stability can be understood by the fact that adsorbed Bi may form chemical bonds with four neighboring Si atoms at the T_4 site rather than with three Si atoms at the H_3 site.

3. Results and discussion

3.1. Au(111), Ag(111) and Sb(111)

Figure 1 shows the electronic band structure of the Au(111) 23-layer slab model calculated without SOC along the 2D BZ lines. The bands are made mostly by folding the bulk ones between Γ and L along the [111] direction of the fcc BZ. Near the Fermi energy, a nearly-free-electron (NFE) parabolic band appears around the $\bar{\Gamma}$ point of the 2D Brillouin zone. This NFE band can be attributed to a surface state (SS) situated inside the bulk bandgap around $\bar{\Gamma}$. The Ag(111) surface reveals similar SS with smaller binding energy to Au(111). With the inclusion of SOC, the SS band in Au(111) shows significant band splitting, as shown in figure 2, being in good agreement with the ARPES experiments [3–5]. The band splitting is confirmed as the spin splitting of the Rashba origin by scaling

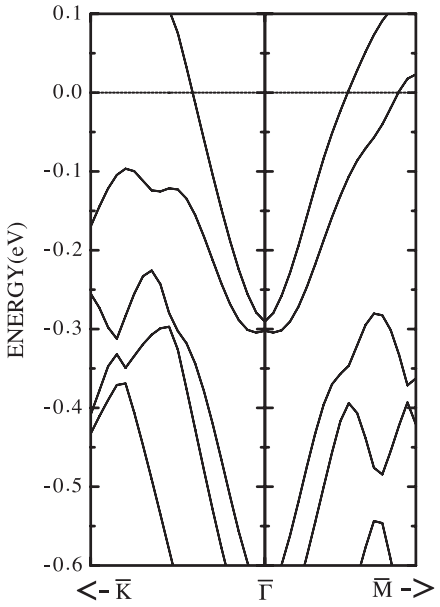

Figure 3. Electronic band structure of Sb(111) calculated with spin–orbit coupling around $\bar{\Gamma}$. Boundaries plotted are $(1/15, 1/15)(2\pi/a)$ on $\bar{\Gamma}\bar{K}$ and $(1/10, 0)(2\pi/a)$ toward $\bar{\Gamma}\bar{M}$, being 1/5 the size of the full zone. The Fermi energy is set to the origin of energy.

Figure 4. The integrand of equation (7) as a function of z along the [111] direction. The surface atom site is taken at the origin.

Table 1. Summary of the Rashba splitting Δk_{R}, spin–orbit coupling parameter ζ_l and orbital angular momentum components of the surface states at Γ in Au(111), Ag(111) and Sb(111). The Rashba splitting is measured as the distance between the bottom of the split bands around $\bar{\Gamma}$.

		$_{71}$Au(111)	$_{47}$Ag(111)	$_{51}$Sb(111)
Δk_{R}	$\bar{\Gamma}\bar{M}$	27.8	—	20.5
(10^{-3} Å^{-1})	$\bar{\Gamma}\bar{K}$	27.8	—	21.2
ζ_l	p	6.34	1.90	2.27
(eV)	d	0.79	0.27	0.52
Component	s	1.3	0.7	3.3
(%)	p	4.7	4.6	9.8
	d	2.5	0.8	—

artificially the magnitude of the SOC parameter ζ_l given in equation (4) and by investigating the spin directions. On the other hand, Ag(111) shows no clear Rashba splitting larger than that by the SS–SS interaction (∼10 meV). The size of the SOC in Ag is about one-third of that in Au. The Ag(111) surface even with artificially magnified SOC comparable to Au shows no Rashba splitting, implying that the Rashba effect comes not only from the strength of SOC.

Before discussing the microscopic mechanism of the Rashba effect, results of band-structure calculations for the Sb(111) surface are presented in figure 3 since Sb has an intermediate size of SOC between Ag and Au. As for Sb(111), Rashba spin splitting is also found around $\bar{\Gamma}$ with almost the equivalent size of the splitting to Au(111). To compare the Rashba effect in Au(111), Ag(111) and Sb(111) surfaces, the size of the spin splitting and SOC are listed in table 1. Since the Rashba splitting appears only around $\bar{\Gamma}$, its measure is represented as the distance between the bottoms of the split bands around $\bar{\Gamma}$. The magnitude of SOC is evaluated with normalized radial functions $R_l(r)$ inside the muffin-tin sphere as

$$\zeta_l = \int_0^{r_{MT}} \hat{\zeta}\, R_l^2(r) r^2 \,\mathrm{d}r. \tag{4}$$

Let us discuss the origin of the Rashba effect at a surface. The SOC Hamiltonian (2) can be divided into two terms according to the momentum component, surface parallel and surface perpendicular, as

$$\mathcal{H}_{\mathrm{SOC}} = \frac{2}{c^2}\left[\left(\nabla V \times \boldsymbol{p}_{\parallel}\right)\cdot\boldsymbol{s} + \left(\nabla V \times \boldsymbol{p}_{\perp}\right)\cdot\boldsymbol{s}\right] \tag{5}$$

and the surface-parallel part can be regarded as the Rashba term $\mathcal{H}_{\mathrm{R}}$. The second term, including the surface-perpendicular momentum component, should be irrelevant to the spin splitting behavior in the 2D band structure. A more general description of the Rashba effect at a surface will be given elsewhere [24]. By assuming a 2D NFE SS with $\boldsymbol{k}_{\parallel} = (k_x, k_y)$ like

$$\psi_{\mathrm{SS}}^{\boldsymbol{k}_{\parallel}}(\boldsymbol{r}) = \mathrm{e}^{\mathrm{i}(k_x x + k_y y)}\phi(z), \tag{6}$$

the Rashba splitting is determined as an integral of the potential gradient along the z direction times the z dependence of the surface wavefunction squared as

$$\begin{aligned}\Delta\varepsilon_{\mathrm{R}} &= \langle\psi_{\mathrm{SS}}^{\boldsymbol{k}_{\parallel}}|\mathcal{H}_{\mathrm{R}}|\psi_{\mathrm{SS}}^{\boldsymbol{k}_{\parallel}}\rangle \\ &= \left|\boldsymbol{k}_{\parallel}\right| \int \mathrm{d}\boldsymbol{r}\frac{2}{c^2}\frac{\partial V}{\partial z}\left|\psi_{\mathrm{SS}}^{\boldsymbol{k}_{\parallel}}\right|^2.\end{aligned} \tag{7}$$

Figure 4 shows the integrand of equation (7) around the surface atom as a function of z calculated for Au(111). It is found that everything happens within one Bohr around the surface atom, where the antisymmetric Coulomb term from the nucleus is dominant in $\nabla_z V$. Such a localized nature of SOC on the Rashba effect has been already pointed out by Bihlmayer *et al* [15]. This means that the asymmetric feature in the z dependence of the surface wavefunction squared $|\phi(z)|^2$ determines the magnitude of the integral in equation (7). The surface wavefunction squared along the z direction is depicted in figure 5 for Au(111), Ag(111) and Sb(111). The asymmetric feature around the surface atom is clearly seen in Au(111) and Sb(111) but is rather small in Ag(111), as expected. It becomes apparent by inspecting the components of the wavefunction because, as shown in table 1, the asymmetric nature of SS in

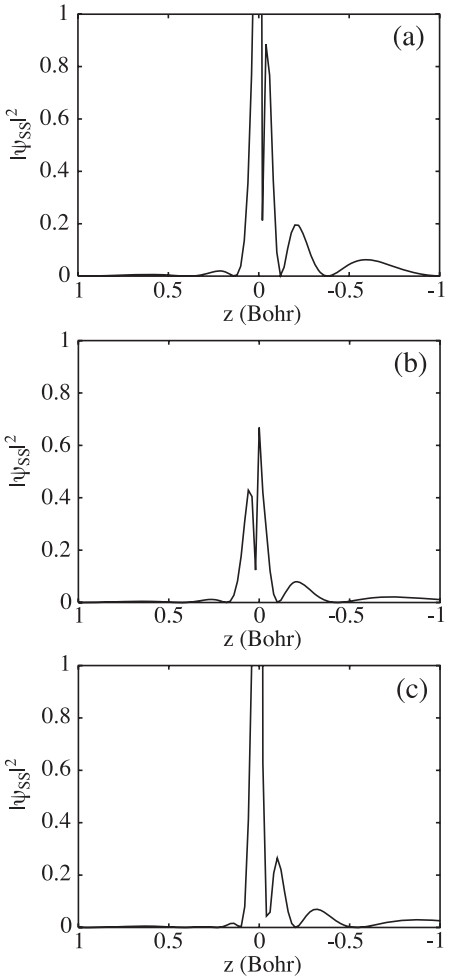

Figure 5. The wavefunction squared of the surface state at $\bar{\Gamma}$ in (a) Au(111), (b) Ag(111) and (c) Sb(111) as a function of z along the [111] direction. The surface atom site is taken at the origin.

Au(111) and Sb(111) originates in the on-site hybridization of the spd and sp orbitals, respectively, at the surface, while SS in Ag(111) is composed predominantly of the p orbital, resulting in a less asymmetric feature. Such on-site hybridization between the orbitals with different parity may be possible by breaking the inversion symmetry at the surface. The d states in Ag are apparently deep and less in SS while those in Au are rather shallow. This different behavior in the d band position is known to come mainly from another relativistic effect, the mass–velocity term.

3.2. Au(110)

Recently, Higashiguchi *et al* have reported an ARPES measurement for Au(110) surface and found an SS-origin dispersion around $\bar{Y}$ without clear Rashba splitting [17, 18]. It is well known that Au(110) undergoes (2 × 1) missing-row surface reconstruction. The surface reconstruction is expected to affect the nature of SS significantly and the resultant Rashba effect may be strongly changed.

Our first-principles electronic-structure calculation for the Au(110) surface with (1 × 1) structure indicates the existence of an NFE-like SS around $\bar{Y}$ about 0.5 eV below the Fermi energy. Anisotropic dispersion in the calculated SS band and the resulting elliptic Fermi surface around $\bar{Y}$ is quite consistent with the ARPES results [17, 18]. With the existence of (2 × 1) missing-row surface reconstruction, an NFE-like SS appears around $\bar{\Gamma}$ just above the Fermi energy. The wavefunctions of SS in Au(110) (1 × 1) and (2 × 1) are depicted in figure 6, together with that in Au(111). It is clearly seen in figure 6 that the surface-normal p orbitals are dominant in SS on all the layers of Au(111). On the other hand, for Au(110) (1 × 1), SS on the outermost surface layer is composed mostly of the surface-parallel p orbitals while the surface-normal p orbitals are found on the second layer. This different character in SS may explain why the band bottom is located at $\bar{\Gamma}$ in Au(111) and at $\bar{Y}$ in Au(110) (1 × 1). In the case of Au(110) (2 × 1), the band bottom of SS moves to $\bar{\Gamma}$ by Brillouin-zone folding. Furthermore, SS has the strongest amplitude on the outermost layer in Au(111), decaying into the bulk exponentially, but the second layer has almost the same amplitude of SS as the outermost surface layer in Au(110) (1 × 1) and (2 × 1).

Figure 7 shows the energy band structure of SS in Au(110) (1 × 1) calculated with SOC. Rashba spin splitting can be seen around $\bar{Y}$. It is quite interesting that the spin splitting is definitely larger for wavevectors from $\bar{Y}$ to $\bar{\Gamma}$ ([001] direction) than for those from $\bar{Y}$ to $\bar{S}$ ([1$\bar{1}$0] direction). This anisotropic feature in the Rashba splitting may be attributed to differences in asymmetric behavior of the corresponding SS around atomic sites near the surface.

Let us consider Rashba splitting generally at the zone boundary. The SOC-origin spin splitting behaviors described solely by the time-reversal symmetry argument may be defined as the *proper* Rashba effect. The time-reversal operation Θ reverses the wavevector and spin simultaneously and the Bloch eigenstate with the time-reversal symmetry is invariant under the operation as

$$\Theta\varepsilon(\boldsymbol{k}, \boldsymbol{s}) = \varepsilon(-\boldsymbol{k}, -\boldsymbol{s}) = \varepsilon(\boldsymbol{k}, \boldsymbol{s}), \tag{8}$$

where $-\boldsymbol{s}$ denotes simply the reverse spin state to $\boldsymbol{s}$. The face center of the zone boundary $\bar{\boldsymbol{C}}$ like $\bar{X}$ and $\bar{Y}$ in the 2D square BZ and $\bar{M}$ in the 2D hexagonal BZ is given as

$$\bar{\boldsymbol{C}} = \frac{\bar{\boldsymbol{G}}}{2}, \tag{9}$$

where $\bar{\boldsymbol{G}}$ is a 2D reciprocal lattice vector, and the time-reversal operation on a state around $\bar{\boldsymbol{C}}$ results in

$$\begin{aligned}\Theta\varepsilon(\boldsymbol{k} + \bar{\boldsymbol{C}}, \boldsymbol{s}) &= \varepsilon(-\boldsymbol{k} - \bar{\boldsymbol{C}}, -\boldsymbol{s}) \\ &= \varepsilon(-\boldsymbol{k} - \bar{\boldsymbol{C}} + \bar{\boldsymbol{G}}, -\boldsymbol{s}) \\ &= \varepsilon(-\boldsymbol{k} + \bar{\boldsymbol{C}}, -\boldsymbol{s}) = \varepsilon(\boldsymbol{k} + \bar{\boldsymbol{C}}, \boldsymbol{s}),\end{aligned} \tag{10}$$

by using the Bloch theorem $\varepsilon(\boldsymbol{k} + \bar{\boldsymbol{G}}, \boldsymbol{s}) = \varepsilon(\boldsymbol{k}, \boldsymbol{s})$ in the second equality. It is, therefore, concluded that the *proper* Rashba spin splitting may take place around the face center of the zone boundary in addition to the zone center ($\bar{\Gamma}$) with the time-reversal symmetry. Note that $\bar{K}$ in the 2D hexagonal BZ is another zone-boundary high-symmetry point but does definitely not meet the condition described above, as discussed in the next section.

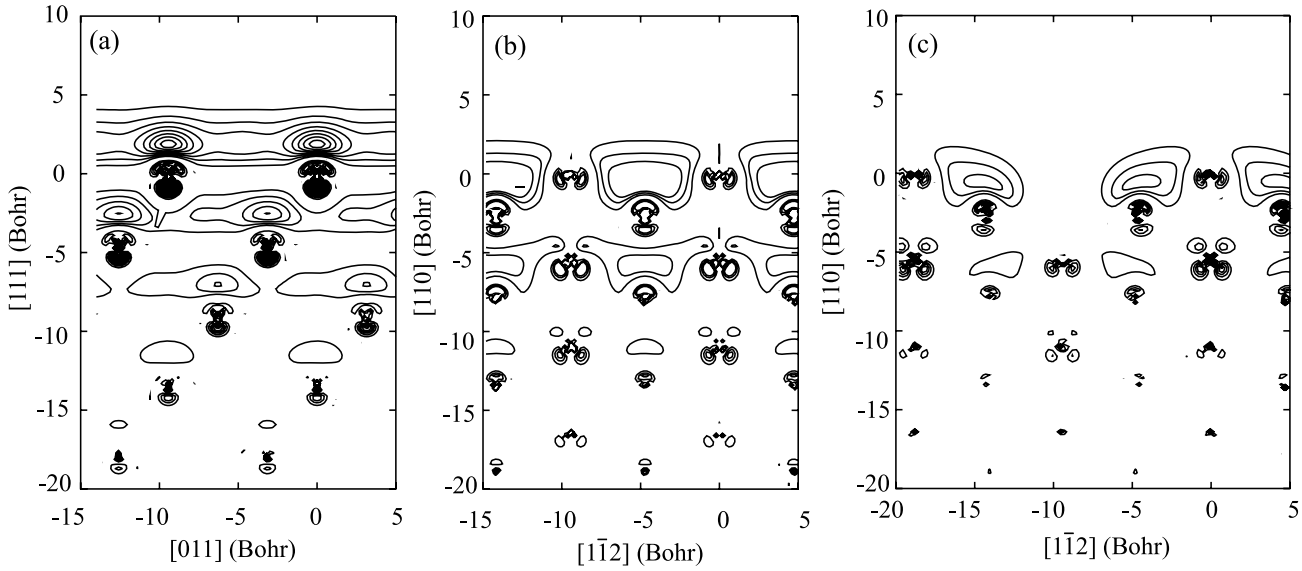

Figure 6. Calculated wavefunction squared of the surface state $|\psi_{SS}^{k_\parallel}|^2$ in (a) Au(111) at $\bar{\Gamma}$, (b) Au(110) (1 × 1) at $\bar{Y}$ and (c) Au(110) (2 × 1) at $\bar{\Gamma}$. The surface-normal is taken along the vertical axis and the surface-parallel direction [110] in (111) and [1$\bar{1}$2] in (110) is along the horizontal axis. The outermost surface layer is located at the origin of the vertical axis. The interval of the contour plot is in 0.0015*e* units.

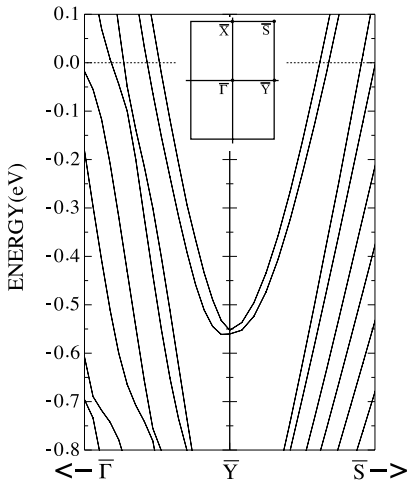

Figure 7. Electronic band structure around $\bar{Y}$ in Au(110) (1 × 1) calculated with spin–orbit coupling. The inset is the corresponding two-dimensional Brillouin zone. Boundaries drawn are $((33/100)(2\pi/b), 0)$ on $\bar{Y}\bar{\Gamma}$ and $((1/2)(2\pi/b), (3/25)(2\pi/a))$ on $\bar{Y}\bar{S}$, where a and $b = \sqrt{2}a$ are the lattice constants of Au(110) (1 × 1). The Fermi energy is set to the origin of energy.

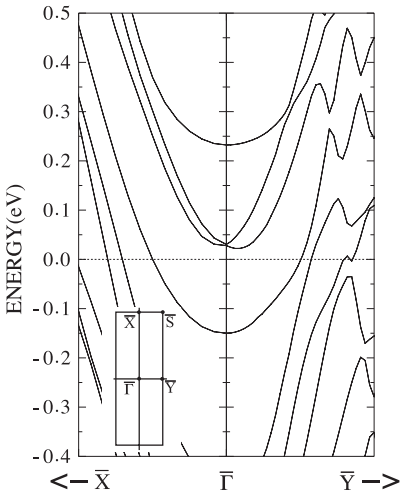

Figure 8. Electronic band structure around $\bar{\Gamma}$ in Au(110) (2 × 1) calculated with spin–orbit coupling. The inset is the corresponding two-dimensional Brillouin zone. Boundaries drawn are $(0, (3/25)(2\pi/a), 0)$ on $\bar{\Gamma}\bar{X}$ and $((33/100)(2\pi/b), 0)$ on $\bar{\Gamma}\bar{Y}$, where a and $b = 2\sqrt{2}a$ are the lattice constants of Au(110) (2 × 1). The Fermi energy is set to the origin of energy.

Figure 8 shows the band structure around $\bar{\Gamma}$ calculated with SOC for the Au(110) surface with (2 × 1) missing-row surface reconstruction. Anisotropic Rashba spin splitting is again found with the same tendency as in Au(110) (1 × 1). In this case, however, an SS with Rashba splitting is located above the Fermi energy around $\bar{\Gamma}$ and may not be observed by the ARPES technique.

3.3. Si(111)-($\sqrt{3} \times \sqrt{3}$)–Bi

A surface system adsorbed with a heavy-element atom is quite interesting for studying the Rashba effect since there might be a possible variation in the system with large SOC. Along such a line, Sakamoto *et al* have observed ARPES spectra for a Bi-adsorbed Si(111) surface with ($\sqrt{3} \times \sqrt{3}$) superstructure [19]. They have found Rashba-type splitting for SS not only around $\bar{\Gamma}$ and $\bar{M}$ but also around $\bar{K}$ in the 2D hexagonal BZ. Concerning the surface structure of Si(111)-($\sqrt{3} \times \sqrt{3}$)–Bi and related adsorbed surface systems, several experimental and theoretical studies have already been reported [20–23] and the adatom position is believed to be at the so-called T_4 site (see figure 9). The Rashba-type spin splitting around $\bar{\Gamma}$, $\bar{M}$ and $\bar{K}$ has been first pointed out by Kinoshita *et al* [21] on the basis of a symmetry consideration.

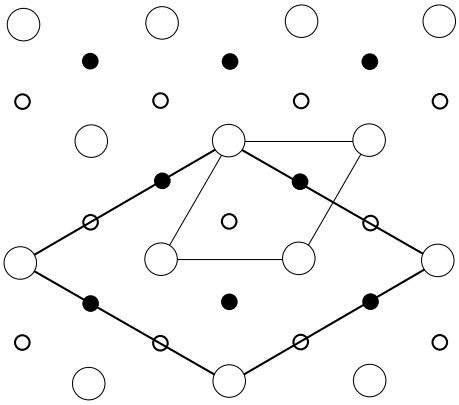

Figure 9. Surface structure of clean Si(111). Small solid, small open and large open circles denote three lateral positions of the double layer named (Aa), (Bb) and (Cc), respectively. The sequence of the double layers in bulk is Aa–Bb–Cc along the [111] direction. When C is the surface layer, the site above (Bb) and (Aa) is called T_4 and H_3, respectively. Thin and thick lines represent the hexagonal unit cell of the (1×1) and $(\sqrt{3} \times \sqrt{3})$ structure, respectively.

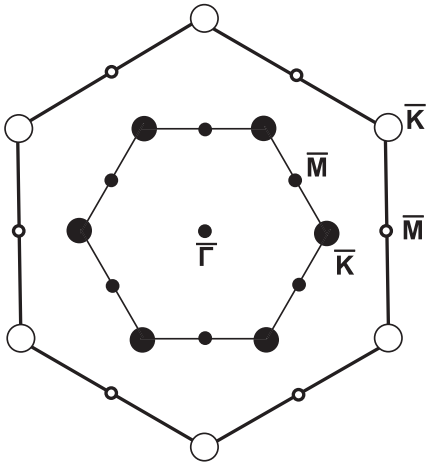

Figure 10. Two-dimensional Brillouin zone of the Si(111) surface. Outer and inner hexagons denote the zone boundary of the (1×1) and $(\sqrt{3} \times \sqrt{3})$ structure, respectively.

The (1×1) and $(\sqrt{3} \times \sqrt{3})$ surface structures of Si(111) are shown in figure 9. The plane groups of the (1×1) and $(\sqrt{3} \times \sqrt{3})$ structures are $p3m1$ and $p31m$, respectively. The difference in the groups comes from the fact whether the mirror planes coincide with the principal axes or not. The corresponding two-dimensional hexagonal Brillouin zones are drawn in figure 10. The coordinates of $\bar{M}$ and $\bar{K}$ are $(1/2, 0)(2\pi/a)$ and $(1/3, 1/3)(2\pi/a)$, respectively, in the 2D hexagonal axes. Note that a wavevector from $\bar{\Gamma}$ to $\bar{K}$ is on the mirror plane for $(\sqrt{3} \times \sqrt{3})$ but out of the mirror plane for (1×1).

Figure 11 shows the energy band structure of Si(111)-$(\sqrt{3} \times \sqrt{3})$–Bi at the T_4 site calculated with and without SOC. Two bands situated inside the energy gaps in the case of no SOC originate in the SS composed mainly of Bi-p and Si-s, p near the surface and reveal Rashba-type spin splitting with SOC. Since the samples experimentally used are n-type, where

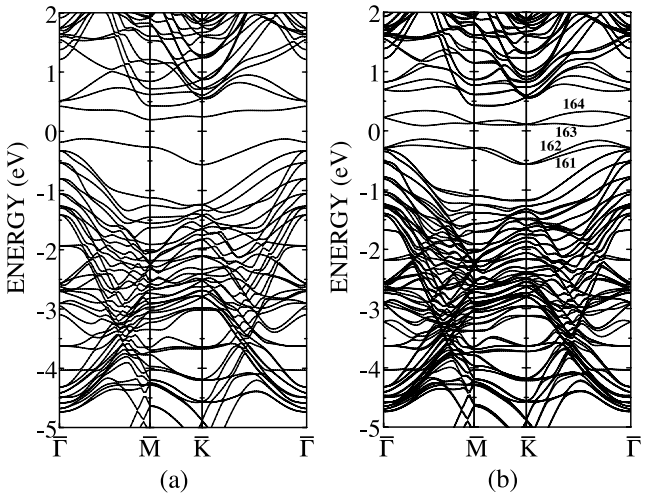

Figure 11. Electronic band structure of Si(111)-$(\sqrt{3} \times \sqrt{3})$–Bi at T_4 calculated (a) without and (b) with spin–orbit coupling. Numbers (#161–164) attached to surface-state bands in (b) denote the band indices.

the chemical potential is located near the conduction band minimum, the SS bands inside the gaps may be observed as occupied bands. In accordance with the ARPES result [19], these two bands are degenerated at $\bar{\Gamma}$, $\bar{M}$ and $\bar{K}$. As mentioned in the preceding section, the Rashba spin splitting around $\bar{\Gamma}$ and $\bar{M}$ can be interpreted solely by the time-reversal symmetry. However, no such simple explanation may be possible for $\bar{K}$. The group of k at $\bar{K}$ is C_{3v} and the irreducible representation of SS at $\bar{K}$ is found to be Γ_1 without SOC and reduced to doubly degenerate Γ_4 by including SOC (see Table 6.5 $3m$ (C_{3v}) of [25]). The double degeneracy of Γ_4 can be considered as of spin degeneracy because its single-group counterpart Γ_1 is a one-dimensional representation with spin degeneracy. As the wavevector is departed from $\bar{K}$ in any direction, no spin degeneracy should be expected since all the representations are one-dimensional (see Table 6.5 m (C_{1h}) of [25]), leading to a *Rashba-like* spin splitting. This *Rashba-like* spin splitting should be referred to as an *improper* Rashba effect in the sense that it cannot be given by the time-reversal symmetry but by the consequence of the double-group symmetry.

The spin expectation values $\langle \boldsymbol{s} \rangle$ of the four split SS bands (#161, 162, 163 and 164) are depicted in figure 12 along the irreducible BZ. It is clearly shown that the spin direction of the SOC-split bands is opposite to each other, mostly on the k_x–k_y plane along all the irreducible BZ lines. It is remarkably interesting to see that the spin direction rotates circularly like vorticity $\nabla \times \boldsymbol{s} \propto \hat{\boldsymbol{k}}_z$ around $\bar{\Gamma}$ and $\bar{K}$ but behaves non-vortical around $\bar{M}$. Another interesting point to be noticed in figure 12 is that the spins are oriented exactly on the xy plane and perpendicular to the irreducible BZ boundaries for the wavevectors on $\bar{M}$–$\bar{K}$ and $\bar{\Gamma}$–$\bar{K}$ but show a finite z component $\langle s_z \rangle$ on $\bar{\Gamma}$–$\bar{M}$. These spin behaviors may be closely related and possibly explained by a symmetry argument with the group of k as follows. There is a mirror symmetry operation, of which the mirror plane includes the z axis, in the group of k on $\bar{M}$–$\bar{K}$ and $\bar{\Gamma}$–$\bar{K}$ but no mirror symmetry on $\bar{\Gamma}$–$\bar{M}$. With

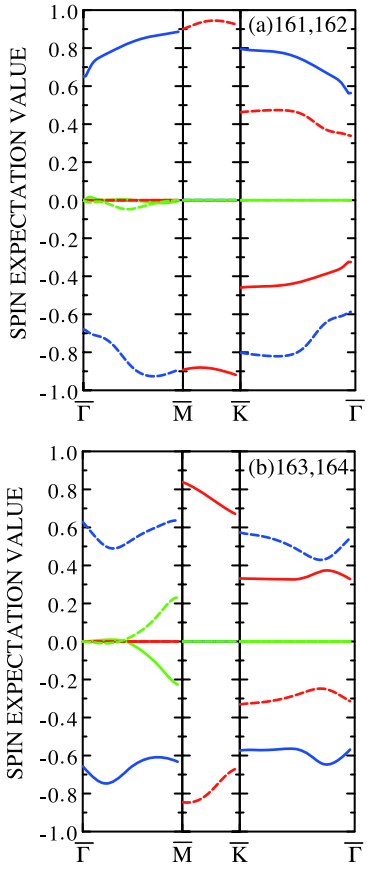

Figure 12. Calculated expectation values of spin angular momentum operator $2\langle s_\alpha\rangle$ ($\alpha = x, y, z$) for the surface-state bands with indices (a) #161 (solid) and 162 (broken), and (b) 163 (solid) and 164 (broken) in Si(111)-($\sqrt{3}\times\sqrt{3}$)–Bi at T_4 along the two-dimensional hexagonal Brillouin zone. Red, blue and green denote the x, y and z components, respectively.

(This figure is in colour only in the electronic version)

respect to the mirror operation, any in-mirror-plane component of SOC, $[\nabla V \times \boldsymbol{p}]_\alpha$, is odd and the wavefunctions are either odd or even. Thus, the matrix element of the in-mirror-plane component becomes zero and the spin expectation value $\langle s_\alpha\rangle$ vanishes, as actually observed for $\bar{M}$–$\bar{K}$ and $\bar{\Gamma}$–$\bar{K}$ in figure 12. Without the mirror symmetry, no such restrictions on the spin direction may be imposed, as seen for $\bar{\Gamma}$–$\bar{M}$ in figure 12. Around $\bar{\Gamma}$ and $\bar{K}$ there are six k lines with the mirror symmetry like $\bar{\Gamma}$–$\bar{K}$ and $\bar{K}$–$\bar{M}$. There are, however, only two k lines with a mirror around $\bar{M}$. Assuming that the spin expectation value $\langle \boldsymbol{s}\rangle$ is continuous and varies slowly in the k space without band crossings, the calculated spin distributions seem to be quite reasonable within the conditions required by the time-reversal and mirror symmetries.

4. Summary

The Rashba effect in several surface systems is studied by using first-principles electronic-structure calculations with the inclusion of SOC. By comparing the Rashba splitting among the Au(111), Ag(111) and Sb(111) systems, the asymmetric behavior of SS along the surface-normal direction is crucial to determine the size of the spin splitting in addition to the magnitude of SOC. Rashba-split SS is seen below (above) the Fermi energy in Au(110)-(1×1) (Au(110)-(2×1)). Anisotropic spin splitting is found and may be attributed to an anisotropic feature of SS. In Si(111)-($\sqrt{3}\times\sqrt{3}$)–Bi, the *proper* Rashba spin splitting is obtained around $\bar{\Gamma}$ and $\bar{M}$ and the *improper* Rashba spin splitting is around $\bar{K}$. The former can be realized solely by the time-reversal symmetry and the latter may be possibly explained by arguments on the basis of the double group of k.

Acknowledgments

The authors thank S Blügel, G Bihlmayer and T Oda for invaluable discussions on the theoretical aspects. They also acknowledge M Higashiguchi, K Shimada, K Sakamoto and A Kimura for providing unpublished experimental data. This work is supported in part by a Grant-in-Aid for Scientific Research in Priority Area 'Development of New Quantum Simulators and Quantum Design' of the Ministry of Education, Culture, Sports, Science and Technology, Japan. The computation in this work has been partly performed using the facilities of the Supercomputer Center, Institute for Solid State Physics, University of Tokyo, and Information Media Center, Hiroshima University.

References

[1] Rashba E I 1960 *Sov. Phys.—Solid State* **2** 1109
[2] Dresselhaus G 1957 *Phys. Rev.* **105** 135
[3] LaShell S, McDougall B A and Jensen E 1996 *Phys. Rev. Lett.* **77** 3419
[4] Reinert F, Nicolay G, Schmidt S, Ehm D and Hüfner S 2001 *Phys. Rev.* B **63** 115415
[5] Nicolay G, Reinert F and Hüfner S 2001 *Phys. Rev.* B **65** 033407
[6] Sugawara K, Sato T, Souma S, Takahashi T, Arai M and Sasaki T 2006 *Phys. Rev. Lett.* **96** 046411
[7] Ast C R, Henk J, Ernst A, Moreschini L, Falub M C, Pacile D, Bruno P, Kern K and Groni M 2007 *Phys. Rev. Lett.* **98** 186807
[8] Nakagawa T, Ohgami O, Saito Y, Okuyama H, Nishijima M and Aruga T 2007 *Phys. Rev.* B **75** 155409
[9] Kirchmann P S, Wolf M, Dil J H, Horn K and Bovensiepen U 2007 *Phys. Rev.* B **76** 075406
[10] Yaginuma S, Nagaoka K, Nagao T, Bihlmayer G, Koroteev Yu M, Chulkov E V and Nakayama T 2008 *J. Phys. Soc. Japan* **77** 014701
[11] Shikin A M, Varykhalov A, Prudnikova G V, Usachov D, Adamchuk V K, Yamada Y, Riley J D and Rader O 2008 *Phys. Rev. Lett.* **100** 057601
[12] Petersen L and Hedegård P 2000 *Surf. Sci.* **459** 49
[13] Koroteev Yu M, Bihlmayer G, Gayone J E, Chulkov E V, Blügel S, Echenique P M and Hofmann Ph 2004 *Phys. Rev. Lett.* **93** 046403
[14] Krupin O, Bihlmayer G, Starke K, Borovikov S, Prieto J E, Döbrich K, Blügel S and Kaindl G 2005 *Phys. Rev.* B **71** 201403(R)
[15] Bihlmayer G, Koroteev Yu M, Echenique P M, Chulkov E V and Blügel S 2006 *Surf. Sci.* **600** 3888
[16] Bihlmayer G, Blügel S and Chulkov E V 2007 *Phys. Rev.* B **75** 195414
[17] Higashiguchi M 2008 private communications

[18] Nuber A, Higashiguchi M, Forster F, Blaha P, Shimada K and Reinert F 2008 unpublished
[19] Sakamoto K 2008 private communications
[20] Northrup J E 1984 *Phys. Rev. Lett.* **53** 683
[21] Kinoshita T, Kono S and Nagayoshi H 1987 *J. Phys. Soc. Japan* **56** 2511
[22] Wan K J, Guo T, Ford W K and Hermanson J C 1992 *Surf. Sci.* **261** 69
[23] Cheng C and Kunc K 1997 *Phys. Rev.* B **56** 10283
[24] Oguchi T and Shishidou T 2008 unpublished
[25] Bradley C J and Crackwell A P 1972 *The Mathematical Theory of Symmetry in Solids* (Oxford: Clarendon)